

<sup>1</sup> PREPARED FOR SUBMISSION TO JINST

<sup>2</sup> **Directional Xenon Measurement**

---

<sup>3</sup> ABSTRACT: Abstract...

<sup>4</sup> KEYWORDS: Only keywords from JINST's keywords list please

<sup>5</sup> ARXIV EPRINT: [1234.56789](https://arxiv.org/abs/1234.56789)

---

<sup>6</sup> **Contents**

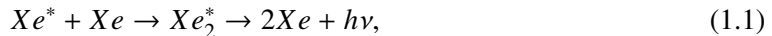
<sup>7</sup> <b>1</b>	<b>Introduction</b>	<sup>1</sup>
<sup>8</sup> <b>2</b>	<b>Experimental Setup</b>	<sup>2</sup>
<sup>9</sup>	2.1 Gas handling system	<sup>2</sup>
<sup>10</sup>	2.2 Cryogenic System	<sup>3</sup>
<sup>11</sup>	2.3 The Detector Chamber	<sup>5</sup>
<sup>12</sup> <b>3</b>	<b>The Data Acquisition (DAQ) System</b>	<sup>7</sup>
<sup>13</sup> <b>4</b>	<b>Simulation</b>	<sup>9</sup>
<sup>14</sup> <b>5</b>	<b>Summary</b>	<sup>9</sup>

---

<sup>15</sup> **1** **Introduction**

<sup>16</sup> The use of Noble-liquid detectors in the field of astroparticle physics has increased in the past  
<sup>17</sup> decades. Detectors aiming at measuring Dark Matter (DM) particles and neutrinos properties use  
<sup>18</sup> large liquid argon or liquid xenon (LXe) chambers [1, 2]. Current and future experiment for DM  
<sup>19</sup> detectioin are tuned to detect weakly interacting massive particles (WIMPs), a postulated candidadte  
<sup>20</sup> for DM particle [3]. LXe based detectors are to date the leading in sensitivity and size for these  
<sup>21</sup> searches [4–7].

<sup>22</sup> When a particle interacts within the LXe media, it forms a cloud of excited and ionized states  
<sup>23</sup> with typical length of 100 nm. The excited Xe ( $Xe^*$ ) combines with other Xe atoms to form an  
<sup>24</sup> excited dimer state (excimer) when they decay to ground state they emit light.



<sup>25</sup> The electrons emitted from the ionization can recombine with a surrounding atom, this process of  
<sup>26</sup> recombination provides another possibility to produce excimers,



<sup>27</sup> Once  $Xe^*$  is produced it adds to the scintillation process explained in 1.1. There are two types of  
<sup>28</sup>  $Xe_2^*$  excimer states, singlet and triplet, with lifetime of  $\sim 3$  ns and  $\sim 25$  ns respectively. The wave-  
<sup>29</sup> length emitted by these states is between (175-180) nm which is lower then the lowest excitation of  
<sup>30</sup> xenon, and therefore travel through it to reach a photo-detector situated outside the LXe. Although

<sup>31</sup> much is measured on these scintillation processes, the basic knowledge of the quantum properties  
<sup>32</sup> of these interactions is based on experiments preformed several decades ago.

<sup>33</sup> The phenomenon of superradiance in which identical quantum states "communicate" through  
<sup>34</sup> electromagnetic field if in close proximity, is well studied. In certain conditions the emission of  
<sup>35</sup> photons from these correlated states is very different than the sum of random states. This difference  
<sup>36</sup> is in spectral, temporal and spatial properties [8, 9]. Early studies show that scintillation in LXe can  
<sup>37</sup> produce coherent amplification of light [10, 11]. These studies were focusing on the macroscopic  
<sup>38</sup> ionization using high energy density electron beams.

<sup>39</sup> The understanding and quantification of the microscopic effects of non linear phenomena such  
<sup>40</sup> as superradiance in Lxe for a single interaction, can improve DM experiments to reduce back-  
<sup>41</sup> ground by the extra knowledge of directionality. irreducible background such as coherent neutrino  
<sup>42</sup> nucleus scattering of neutrinos from the sun can be discard.

<sup>43</sup> In this paper we present an experimental set-up called DIREXENO (Directional Xenon) aiming  
<sup>44</sup> at measuring the spatial distribution of LXe scintillation light, and quantify non-isotropic emis-  
<sup>45</sup> sion.

## <sup>46</sup> 2 Experimental Setup

<sup>47</sup> The experimental setup that is described in this section, is designed to measure, the properties of  
<sup>48</sup> LXe scintillation. However it is designed in a modular way, so it can serve different requirements  
<sup>49</sup> from different future experiments. There are three main building blocks consisting the full setup,  
<sup>50</sup> The purification and circulation system, the cryogenic system, and the detector system. Each build-  
<sup>51</sup> ing block can be replaced without effecting the others, this concept as well as some design ideas  
<sup>52</sup> were taken from [12]. The full assembly (figure. 1) is held on three separate wracks, one for the  
<sup>53</sup> DAQ, while the two others which hold the the detector and purification system are joined using a  
<sup>54</sup> 100mm bar with shock absorbers on both sides.

### <sup>55</sup> 2.1 Gas handling system

<sup>56</sup> A typical LXe detector must keep a high level of purity. Careful selection and meticulously clean-  
<sup>57</sup> ing of all parts before mounting, is needed, however is not sufficient. The desired level in most  
<sup>58</sup> detectors of impurity concentration is at the level of 1 ppb  $O_2$  equivalent [1]. This is crucial to  
<sup>59</sup> allow ionization electrons drift for several cm. To reach that level in a reasonable amount of time  
<sup>60</sup> (several days instead of months), continuous purification is needed. The gas system, provides this  
<sup>61</sup> process, alongside with all gas handling operations such as filling and recuperation.

<sup>62</sup> During purification mode, xenon is taken from the chamber (in liquid phase) passes through  
<sup>63</sup> a heat exchanger<sup>1</sup> where it is heated and vaporized. Then the xenon is forced by a KNF diaphragm  
<sup>64</sup> pump into a hot getter<sup>2</sup> which cleans the xenon from most impurities. The xenon also passes  
<sup>65</sup> through an MKS Mass Flow Controller<sup>3</sup> (MFC) which enables the monitoring of heat load.

---

<sup>1</sup>GEA GBS100M-24 plate heat exchanger

<sup>2</sup>MONO-TORR PS4-MT15-R-2

<sup>3</sup>MKS mass flow controller

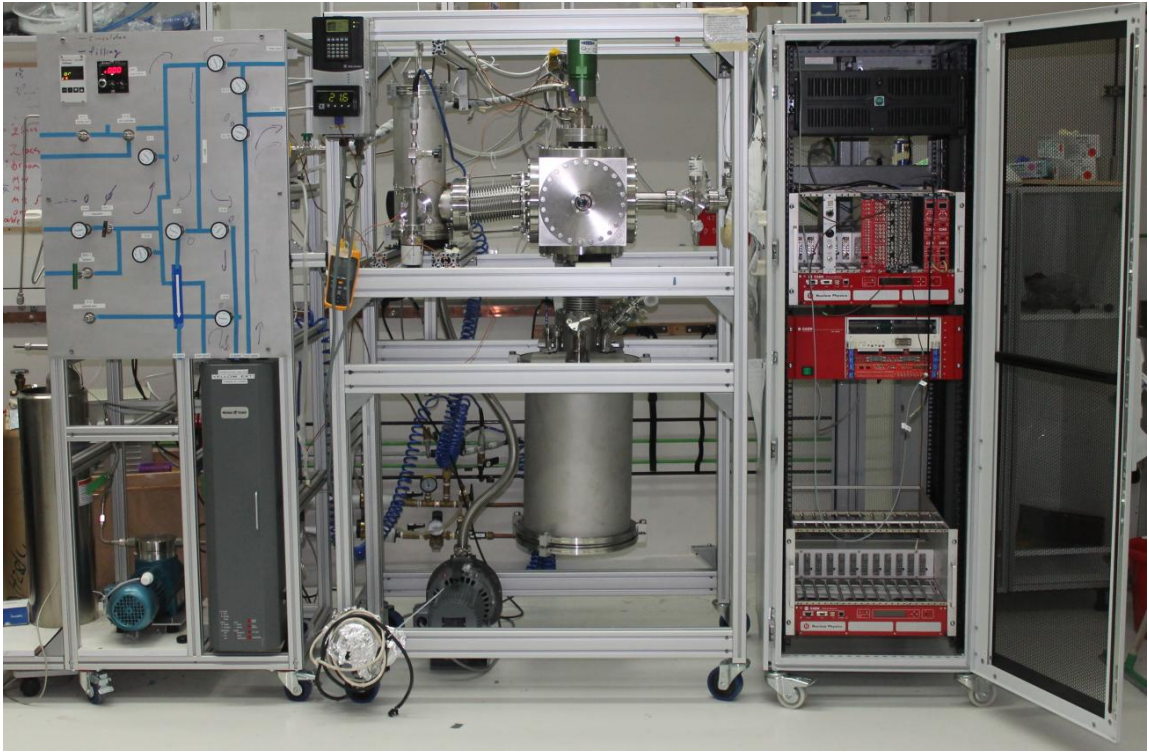


**Figure 1.** Direxeno. On the left the purification system, in the middle the cryogenic and detector chamber, and on the right the Data acquisition system.

66 After the xenon is purified, it is delivered back to the cryogenic system through the heat ex-  
 67 changer, there most of the xenon gas is liquefied before it continues back to the chamber. A  
 68 schematic of this system is shown in fig. 2.

## 69 2.2 Cryogenic System

70 Remote cooling is generally used in DM experiments due to background radiating from the cooler  
 71 to the detector. Although in our system this is not of great importance there are still several ad-  
 72 vantages to remote cooling such as: lowering acoustic noise from the cryo-cooler and flexibility to  
 73 design changes. The cryogenic system is connected on one side to the gas system and on the other  
 74 to the detector chamber, any change in the system (e.g., cooler type or model) requires the change  
 75 of that specific part without changing the detector nor the gas system.

76 The system is made out of two chambers, the outer vessel (OV) which holds the insulation  
 77 vacuum, and the inner vessel (IV) which holds the xenon. In addition to the vacuum which prevents  
 78 heat leaks from diffusion and convection, the entire IV is covered by multi layer aluminized Mylar  
 79 to prevent heating via radiation. A picture of the detector and the CAD design are shown in Fig 3.

80 The OV is made of a 10" CF cube, with ports on all six faces (e.g., electrical feedthroughs,  
 81 pumping ports, view ports, etc.). The space between the OV and IV is held constantly in vacuum  
 82 for heat insulation. This vacuum is shared with the detector and with the heat exchanger chamber  
 83 via 6" CF flexible bellows.

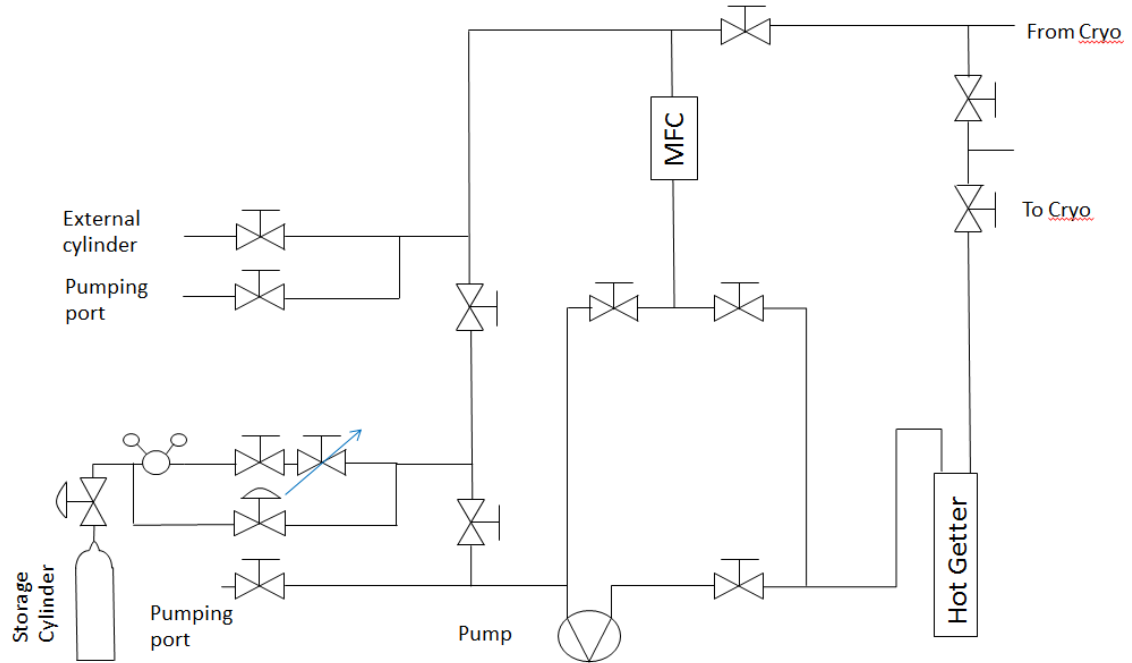


**Figure 2.** Schematics of the purification system. High pressure valves are indicated as valves with arcs. Needle valves are indicated as a valve with an arrow.

84        The IV is made of XXX cm height cylinder with 6" CF flanges on the top and bottom parts of  
 85        it, and it holds inside xenon. A XXX " cold finger is welded to the top flange of the IV. The design  
 86        of the cold finger is similar to the design of [13], the inner part of the cold finger is made of long  
 87        fins, therefore the surface area of it is bigger resulting in a better heat transport. The upper part of  
 88        the cold finger is in thermal contact with the cryo-cooler<sup>1</sup> via a cooper adapter. The copper adapter  
 89        holds two  $100\Omega$  pt resistor which are connected to a PID reader<sup>2</sup> fot temperature measurements. A  
 90        Cartridge-heater is also inserted to the copper adapter for emergency heating.

91        The cryo-cooler provides up to 70 W of cooling power, and is connected via a 4 1/2" to  
 92        10" reducer to the OV from above, and reaching the IV top flange. Common cryo-coolers used  
 93        for xenon experiments, work in maximal cooling mode permanently. The QDrive, instead, has  
 94        temperature control allowing it vary the cooling power, which enables to set the temperature with  
 95        fluctuations smaller then 0.1 C° on the cooler itself.

96        On the inner side of the bottom flange of the IV a thin SS funnel is installed collecting all LXe  
 97        drops from the cold finger, and delivering them to the detector part. This flange is connected to the  
 98        detector part, via a 3 3/8" flexible bellows. This bellows hosts two small pipes (1/4") connected to  
 99        the circulation system, and a third pipe coming from the funnel, all three pipes deliver LXe whereas  
 100      the GXe is filling the bellows.

<sup>1</sup>QDrive 20BB 9p6 A 3 AYNBNCO

<sup>2</sup>cryo-con model 18i Cryogenic Temp Monitor

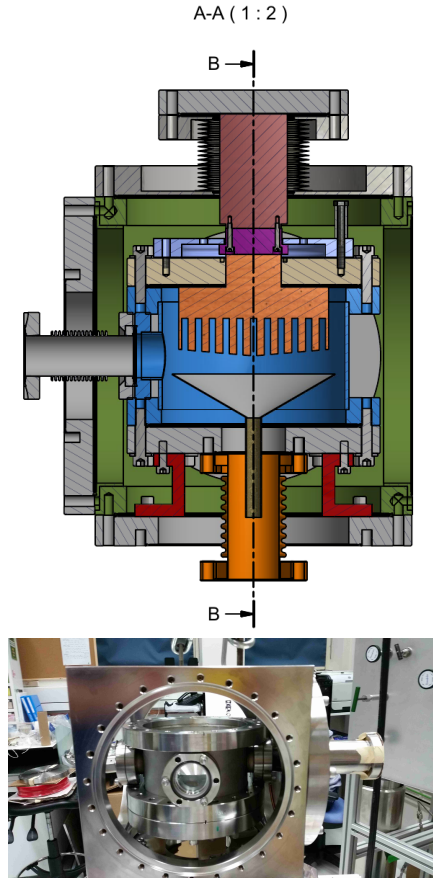


**Figure 3.** (Top) CAD view of the cryogenic system. (Bottom) Picture of the cryogenic system.

### 101 2.3 The Detector Chamber

102 The Detector chamber refers to the whole apparatus below the cryogenic system. It is built such  
 103 that apart from the interface to the cryogenic system, it can be changed and modified easily for  
 104 future experiments. The interface unit is built out of 2 flanges welded together via 7 tubes, which  
 105 serve as service ports for electrical and other feedthroughs. The upper flange, ISO-K 160, is part of  
 106 the outer vessel and shares the insulation vacuum of the cryogenic system, the inner one , CF-8",  
 107 is part of an inner vessel for future detectors, and would hold xenon inside. For our experiment we  
 108 modified the CF flange to fit also a XXX" CF flange which we use.

109 The OV is closed with a cylinder XXX cm height closed from the bottom with another ISO-  
 110 K 160 flange, the height of the cylinder is determined such that the maximal height of the whole  
 111 apparatus is 190 cm, allowing the mobility of the detector through standard doors.

112 The XXX" CF flange is connected to a closed vessel internally divided into two parts. This  
 113 vessel serves as a xenon reservoir. The two parts of the vessel are connected to a spherical orb from  
 114 above (inner part) and from below (outer part). LXe is circulated such that new LXe drips into the  
 115 outer part and pumped from the inner one. This way the liquid level is controlled, and the sphere  
 116 itself will always be filled with LXe.

117 The main part of the detector is the spherical orb, which is made of fused silica. In the center

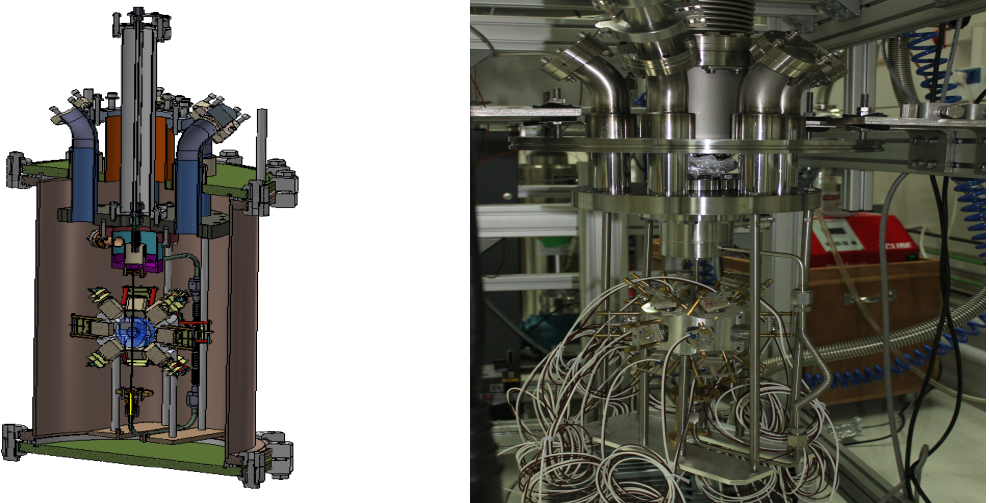


**Figure 4.** (Left) CAD design of the detector part. (Right) The detector chamber open, in the middle is the PMT holder.

118 of it, a smaller sphere is curved to hold the LXe, two invar pipes are connected to it from the top  
 119 and bottom with SS mini-CF flanges at the end, to circulate the xenon (see Fig. ??). The sphere  
 120 stands in the center of 20 PMTs<sup>1</sup> to detect light emitted from the LXe.

121 The bottom flange of the sphere is held using a brass holder to prevent force or torque applied  
 122 on the sphere while mounting the detector. The brass holder is connected to a plate held from the  
 123 top 8" flange, and is also used to align this plate at first installation.

124 The xenon sphere should be as large as possible however not too large to avoid double scatters.  
 125 The fused silica sphere should be large enough in order to reduce internal reflections, but not too  
 126 large to attenuate the scintillation light. The sphere is produced from HPFS 8655 Fused Silica.  
 127 The refractive index of this material is 1.575 whereas of the LXe is 1.61, this prevents change in  
 128 directionality when the light travels from the LXe to the fused silica. The measured transmittance  
 129 of the HPFS is 99.75 %cm, hence almost no light is absorbed in it.

130 The 20 PMTs are held with a special aluminum holder, coated with anti-reflection substance.  
 131 The holder is made of two hemispheres hosting the PMTs in 3 rows all of them pointing to the  
 132 center of the fused-silica sphere. The PMTs are held only via their bases. The bases are held using  
 133 M2 PEEK screws. In Fig. 4 is a CAD and real view of the detector part.

134 The sources that will be used for exciting the xenon, and creating the superradiance (signal)  
 135 as well as the standard emission (background), will be  $^{137}\text{Cs}$  (662 keV) and  $^{57}\text{Co}$ (122keV & 136  
 136 keV) for ER and  $^{241}\text{AmBe}$ , D-D neutron generator, or neutron produced in an accelerator for NR  
 137 . The mean free path for this energy is a couple of mm ( $^{57}\text{Co}$ ) and 0.5-3 cm ( $^{137}\text{Cs}$ ), therefore a  
 138 diameter of 2cm was decided for the small sphere. For The large sphere GENAT4 simulation were  
 139 used. Simulating 178nm photons randomly in the xenon and checking the ratio of detection. For  
 140 the 99% transmittance it is clear that the radius should be around 3 cm, see Fig. ??.

---

<sup>1</sup>r8520-406 Hamamatsu 1" PMT

141 **3 The Data Acquisition (DAQ) System**

142 In this section we discuss the data acquisition and readout from the PMT channels. We use a  
143 heterogeneous system consisting of both NIM and VME electronics modules, with the data readout  
144 being carried out through the VME controller module V2718 and a PCIe card A3818.

145 The schematic layout of the DAQ system is shown in Fig. 5. All the 20 PMTs are oriented in  
146 the holder assembly which was discussed in section—. The PMTs are ramped up to +800V (the  
147 maximum is +900V) using a 24 channel VME high voltage distributor module (VDS18130p) from  
148 iseg. The voltage is monitored by the GUI based control software provided by iseg. For clarity in  
149 understanding, we term the raw electrical pulse output of the PMTs as  $S_i$  (raw),  $i = 1 - 20$ . These  
150 raw pulses are then amplified and shaped using two NIM photomultiplier preamplifiers (Phillips  
151 776). Each of the preamplifier model provides 16 independent and direct-coupled amplifiers chan-  
152 nels. The preamplifier channels operate from DC to 275 MHz and produce two identical  $50\ \Omega$  non  
153 inverting outputs with voltage gains of 10. We term the amplified pulses as  $S_i$ ,  $i = 1 - 20$ . One of  
154 the two identical analog outputs from each channel is being converted to a digital signal with an  
155 Analog to Digitizer converter (ADC V1742).

156 The ADC module V1742 is a VME board with two 12bit 5GS/s Switched capacitor Digitizer  
157 sections, each of them with 16+1 channels, based on DRS4 chip. The dynamic range of the input  
158 signal is 1 Vpp with adjustable DC offset. This module can sample either bipolar or unipolar  
159 analog input signal within the dynamic range in a circular analog memory buffer, with default  
160 sampling frequency choices 5GS/s, 2.5 GS/s or 2 GS/s. As soon as a trigger signal reaches, all the  
161 analog memory buffers get frozen and then gets digitized into a digital memory buffer with a 12  
162 bit resolution.

163 We generate an intrinsic trigger for the system, with the coincidence of any two out of the  
164 twenty PMTs. The second output from the preamplifier channels are converted to binary signals  
165 using two 16 channel leading Edge discriminator (V895). In Fig. 5, we term the binary outputs  
166 from V895 as  $SD_i$ ,  $i = 1 - 20$ . The  $SD_i$  signals are then passed over to V1495, an FPGA based  
167 General purpose VME board which is programmed to perform the logic operation to obtain the  
168 trigger. At present, the coincidence of any two out of the twenty PMTs forms the trigger logic. The  
169 output of V1495 logic operation is used to trigger the ADC V1742 module. In order to record the  
170 PMT noise rate, the  $SD_i$  signals are duplicated and fed to a scaler V830.

171 The PMT event information and the trigger rate are read from the ADC, while the Scaler  
172 records the PMT noise rate. The data readout to the acquisition PC is done through the Controller  
173 and optical link to the master PCIe card. The further analyses of the relevant events in the PMTs  
174 will be carried out offline using an analysis framework.

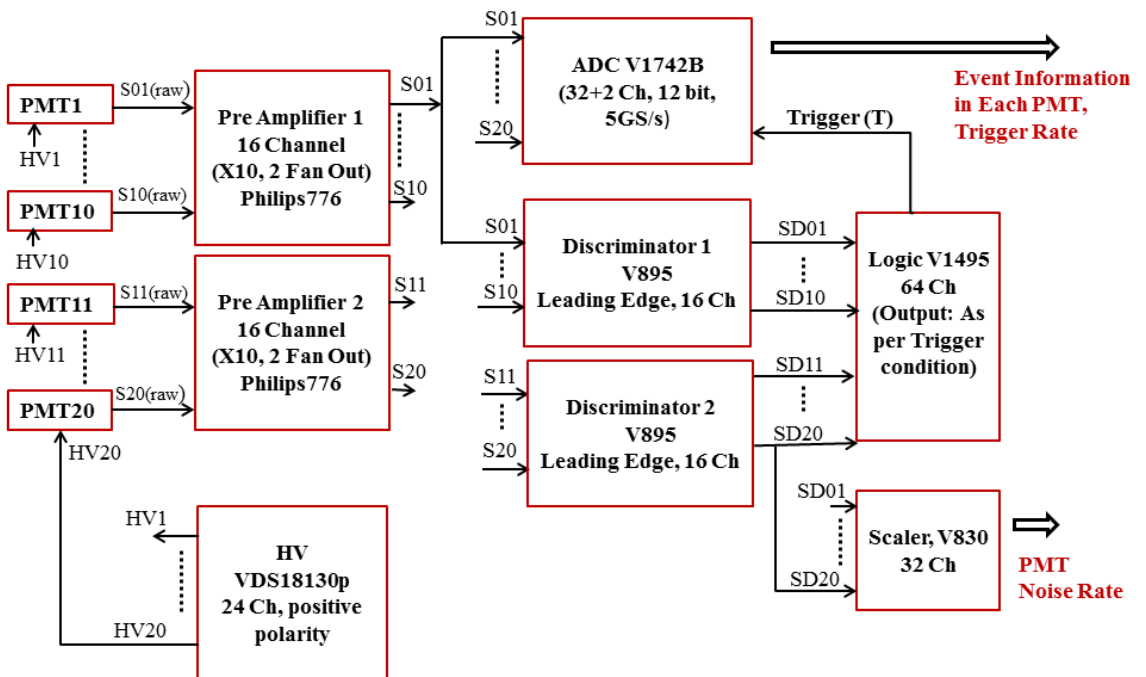


**Figure 5.** The schematic of the Data Acquisition System of Direxeno. It consists of 20 PMTs and the subsequent electronic channels to record the events for an internal trigger generated by the coincidence of any two PMTs in the system and also the PMT noise rate.

175 **4 Simulation**

176 **5 Summary**

177 **References**

- 178 [1] E. Aprile and T. Doke. Liquid Xenon Detectors for Particle Physics and Astrophysics. *Rev. Mod.*  
179 *Phys.*, 82:2053–2097, 2010.
- 180 [2] A. Rubbia. Future liquid Argon detectors. 2013. [*Nucl. Phys. Proc. Suppl.* 235-236, 190(2013)].
- 181 [3] J. Silk et al. *Particle Dark Matter: Observations, Models and Searches*. Cambridge Univ. Press,  
182 Cambridge, 2010.
- 183 [4] E. Aprile et al. First Dark Matter Search Results from the XENON1T Experiment. 2017.
- 184 [5] D. S. Akerib et al. Results from a search for dark matter in the complete LUX exposure. *Phys. Rev.*  
185 *Lett.*, 118(2):021303, 2017.
- 186 [6] Changbo Fu et al. Spin-Dependent Weakly-Interacting-Massive-ParticleâŠNucleon Cross Section  
187 Limits from First Data of PandaX-II Experiment. *Phys. Rev. Lett.*, 118(7):071301, 2017.
- 188 [7] J. Aalbers et al. DARWIN: towards the ultimate dark matter detector. *JCAP*, 1611:017, 2016.
- 189 [8] R. H. Dicke. Coherence in spontaneous radiation processes. *Phys. Rev.*, 93:99–110, Jan 1954.
- 190 [9] M. Gross and S. Haroche. Superradiance: An essay on the theory of collective spontaneous emission.  
191 *Physics Reports*, 93(5):301 – 396, 1982.
- 192 [10] N G Basov, V A Danilychev, and Yurii M Popov. Stimulated emission in the vacuum ultraviolet  
193 region. *Soviet Journal of Quantum Electronics*, 1(1):18, 1971.
- 194 [11] Frederick H. Mies. Stimulated emission and population inversion in diatomic bound-continuum  
195 transitions. *Molecular Physics*, 26(5):1233–1246, 1973.
- 196 [12] K L Giboni, X Ji, H Lin, A Tan, T Ye, Y Zhang, and L Zhao. A liquid xenon development and test  
197 system. *Journal of Instrumentation*, 9(04):T04006, 2014.
- 198 [13] E. Aprile et al. The XENON100 Dark Matter Experiment. *Astropart. Phys.*, 35:573–590, 2012.